

# ANALYSIS OF BIOMEDICAL FILTER PARAMETERS USING CT IMAGES

Mamatha R<sup>1</sup>, Sharavathi M H<sup>2</sup>

<sup>1,2</sup>Assistant Professor, Dept of ECE, Government S. K. S. J. T. I, Bangalore  
mamathasairam@gmail.com, mhsharavathi06@gmail.com

## Abstract

The analysis and enhancement of biomedical images are crucial for accurate diagnosis and treatment planning. This study focuses on the evaluation of biomedical filter parameters using CT images, emphasizing the Gamma correction method and Homomorphic filtering. Gamma correction is utilized to adjust image luminance, thereby enhancing contrast and improving the visibility of critical anatomical structures. By varying the gamma values, we tailored the image quality to specific diagnostic needs, such as distinguishing between soft tissues and bone structures. Homomorphic filtering, meanwhile, addresses the dual challenge of contrast enhancement and noise reduction by transforming the image into the logarithmic domain and separating illumination from reflectance. This method significantly improved image clarity and consistency by standardizing lighting conditions. Our comparative analysis demonstrates that both Gamma correction and Homomorphic filtering offer substantial benefits for biomedical image enhancement, each with unique strengths. Gamma correction provides flexible, user-defined contrast adjustments, while Homomorphic filtering excels in mitigating lighting inconsistencies and noise. The findings highlight the potential for these techniques to enhance diagnostic accuracy and suggest avenues for further research into their integration and optimization in automated imaging systems.

Keywords: Biomedical, CT, Filters, Image Processing, Pre-processing

## 1. Introduction

The evolution of medical imaging and computer-aided diagnosis (CAD) provides an alternative solution towards compensating the difference in patient versus an experienced doctor's gap. There are many medical imaging modalities, including X-ray, MRI, tomography, CT-scan, ultrasonography, and mammography. Each of these medical images is subjective and applicable to different situations. However, CT scan is more preferred than the rest of medical imaging when it comes to brain tumour analysis and diagnosis. It provides a high-resolution representation of the human brain that offers effective visualization, essential for in-depth analysis for diagnosing, treating, and monitoring brain diseases. CT scanned images are often corrupted with imaging artifacts during brain scanning, signal interferences, CT scanning machine vibration, and patient motions. This degradation factor affects the diagnosis process and creates a challenging problem in analyzing brain images for tumour classification. Therefore, the medical image contrast enhancement method plays a vital role in obtaining high-quality brain diagnosis images. Many prior art techniques are available to repair damaged contrast features and improve their visual quality to overcome the human visual system's weaknesses. The medical enhancement process is carried in two types of domain, i.e., spatial and frequency domain techniques. Most of the existing techniques are found to provide excellent image contrast, but also they suffer from producing an unnatural appearance by the over-enhancing visual feature of the image. Also, the prior art has a common disadvantage that they cannot maintain image contrast luminance.

## 2. Survey on existing systems.

The pre-processing operation on the medical image has a significant role in enhancing medical image quality for abnormalities detection and classification. However, various image enhancement techniques are developed by the research community. This section presents a review study intended to determine the research pattern's progress towards Brain CTS image enhancement.

Improvement of the visual quality of CTS images from poorly degraded resolution is quite a challenging task. The work carried out by the authors of [19] have introduced a framework of multi-contrast CTS image enhancement using gradient value relationship between various contrast factor of input images, to reconstruct a high-resolution image which is further obtained by using the iterative approach of the back-projection filter. The study outcome illustrates the presented approach's effectiveness, validated using synthetic and real brain CTS images. The presented approach's performance is better compared to existing similar approaches in terms of high visual resolution.

The work of authors of [17] has discussed the image enhancement techniques based on wavelet decomposition, and they have addressed the problem associated with the computing time of such techniques. To provide effective enhancement and processing time efficient mechanism, the authors have introduced an improved mechanism based on the wavelet decomposition, which uses the information from the high-frequency sub-band images decomposed by the biorthogonal type wavelet filter. The study outcome demonstrates that the presented enhancement mechanism efficiently improves the image's quality by taking less computation time.

After reviewing the existing literature, it is analyzed that many research studies have shown their interest in the analysis and detection of brain tumors. The current research focuses more on brain images with high visual quality, but they are not worried about CTS images with low visual quality. Hence, research efforts, especially towards visual quality enhancement of brain MRI, are missing in the existing literature. It has found that maximum research studies for segmentation and tumour classification consider the brain image as a database, which is considered to be mostly undisputed and noise-free. However, in real-time brain CTS images for tumour recognition and classification, such research work's efficiency and applicability are limited. Hence, the existing literature's contribution is insufficient to bring effective and quality-aware visualization subjected to both human visual perception and CAD system for brain detection and identification of tumours from MR brain image. The aim of this research paper is to develop a straightforward novel framework capable of enhancing the pre-processing operation of brain CTS images.

### 3. Proposed framework:

The proposed framework's primary purpose is to suggest a qualified optimal model that can provide full image visual quality enhancement for a given set of brain CTS images. The proposed system also contributes to ensuring that a highly adaptive interface model is built to perform a complete image enhancement on any brain image. This model is also designed to provide a time-efficient mechanism to diagnose brain MRI images deeply with less effort.

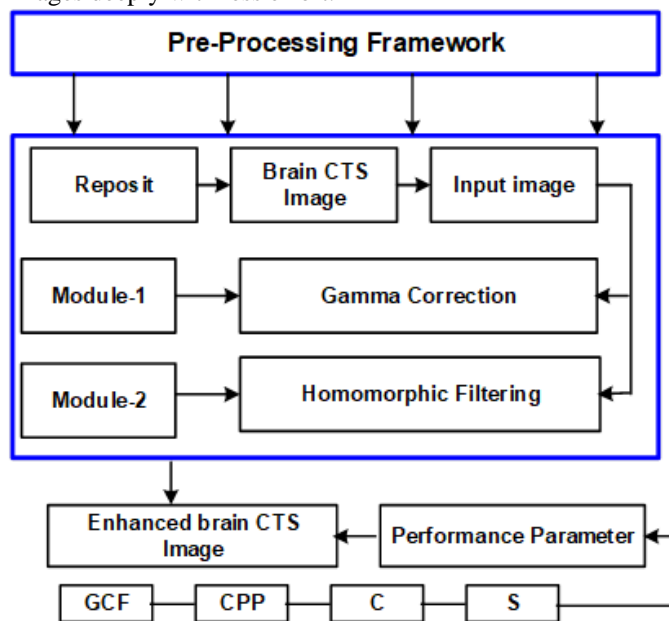


Figure-1: Proposed image enhancement framework

The proposed image enhancement framework design consists of multiple modules, as shown in Figure-1. The first module of the framework carries image enhancement process using gamma correction, the second module of the proposed framework performs Homomorphic filtering operation on the gamma-corrected image. This method's primary interest is its simplicity and durability for visual quality enhancement performance for the given input medical image. The proposed system's accuracy

and efficiency are evaluated in terms of GCF (Global Contrast Factor), CPP (Contrast per Pixel), Contrast, and Sharpness.

This section presents the methodology adopted in the proposed system to convert an input CTS image visually pleasing by enhancing the contrast and brightness feature to acquire comprehensive analysis without visual impairments. The proposed work employs a multi-layered approach, as shown in Figure-1, which determines the transformation function based on the input brain CTS image's characteristics. The interpretations of each methodology are described, followed with computational steps as follows:

#### Gamma Correction:

Gamma correction refers to the controls function responsible for representing the image's overall brightness, which appears to be bleached or too dark. The logic behind the gamma correction technique is to apply a transformation function to the input image so that, contrast factor of the output image is enhanced based on two varying parameters or variables such as  $c$  and gamma value  $\gamma(Y)$  between 1.01 to 2.

Thus, gamma can be expressed as a nonlinear relationship between the input - (pixel value) and the resulting output (i.e., brightness or loosely called intensity). The gamma correction transform is given by a functional relationship, which can be expressed as:

$$I_{Out} = c I_{In}^{\gamma} \dots (1)$$

The equation (1),  $c$  and  $\gamma$  indicate a parameter value used to adjust the transformation function's shape.  $I_{Out}$  represents resultant image intensity values (i.e., output image), and  $I_{In}$  represents pre-compensation image data. The parameters  $c$  is mostly considered a constant equal to one, and the value of  $\gamma$  varies with different ranges, which generates different stretching effects. The proposed study considers the assignment of gamma value between suitable ranges, i.e., 1.01 to 2. However, the gamma correction sometimes produces an assorted result as it pre-assigned gamma value for each input image. Therefore, the proposed system performs an optimization of gamma correction mechanism to improve the image's visual quality to acquire enhanced contrast ratio as a pre-processing step. Besides, the optimization approach is implemented by the varying value of gamma from the range between 0.9 to 1.2, which is selected based on the statistical characteristics of each input image. The computing steps for implementing Gamma correction are as given below:

#### Computing Procedure for Gamma Correction

##### i). Loading Input value

Step-1. Initialize  $I_m(\text{Input image}) \rightarrow \text{global}$

Step-2. Load Image from database

Step-3. Read  $\rightarrow$  Image

Step-4. Perform of RGB image to Grayscale Image conversion

a. Check : size of Input image = 3

b. Convert: Input image to gray

Step-5. Display Input image

##### ii). Applying Gamma Correction

Step-6. Initialize variable  $I_{\gamma}$

Step-7. Assign  $I_{\gamma} \rightarrow \text{double}(I_m)$

Step-8. Assign Value for  $\gamma$

a.  $\gamma \rightarrow$  Select between a range of 0.01 to 2

Step-9. Compute  $I_{\gamma} \rightarrow (I_{\gamma})^{\gamma}$

Step-10. Perform Normalization  $\leftarrow I_{\gamma}$

Step-11. Compute GCF, CPP, Contrast, and Sharpness

**iii) Optimization of Gamma Corrected Image**

Step-12. Initialize variable  $v1, v2, v3, v4, T \rightarrow \text{Global}$

Step-13. Create empty matrix  $[] \leftarrow v1, v2, v3, v4, T$

Step-14. For each value of  $\gamma$  between 0.9 to 1.2

Step-15. Repeat the above process ("Step6 to Step11")

Step-16. Assign  $GCF \rightarrow v1, v2 \rightarrow CPP, v3 \rightarrow \text{Contrast}, v4 \rightarrow \text{Sharpness}$

Step-17. Store value of  $\gamma$  with respect to  $v1, v2, v3, v4 \rightarrow T$

Step-18. Perform Reconstruction of  $v1, v2, v3, v4$

Step-19. Select an optimal mechanism

$V \rightarrow [v_{R1}; v_{R2}]^{\text{Transpose}}$

$S \rightarrow fs(V, 2)/2$

Step-20. Compute the best index( $b_i$ )

$b_i \rightarrow S == \text{fmax}(S)$

$\gamma_i \rightarrow T(b_i, I)$

Step-21.  $I_{\gamma \text{Opt}} \rightarrow (I_{\gamma})^{\gamma_i}$

Step-22. Perform Normalization  $\leftarrow I_{\gamma \text{Opt}}$

## Homomorphic Filtering

Homomorphic filtering is a method for recovering a degraded image having uneven illumination due to a multiplicative random signal. The concept of homomorphic filtering in the proposed framework utilizes an illumination-reflection model in the image enhancement process. This model considers that an image is an array of measured light intensities and is a function of the total light reflected by an object in the scene. The following are the essential and sequential steps taken in the proposed filtering operation on the input brain MR image.

i. Designing a filter

ii. Execute the logarithm function to perform the transformation of the input image into the frequency domain.

$$ZI_m(x, y) = \log t(x, y) + \log \rho(x, y) \dots (\text{eq.2})$$

iii. Applying Fourier transforms.

$$ZI_m(u, v) = FT t(u, v) + FT \rho(u, v) \dots (\text{eq.3})$$

iv. Obtain filtered input image by passing a transformed image from the constructed filter.

$$FT I_m(u, v) = H_{mf}(u, v) ZI_m(u, v) \dots (\text{eq.4})$$

$$FT I_m(u, v) = H_{mf}(u, v) \cdot FT t(u, v) + H_{mf}(u, v) \cdot FT \rho(u, v) \dots (\text{eq.5})$$

v. Transformation of the filtered image into the spatial domain

$$FT I_m(x, y) = FT^{-1} \{ H_{mf}(u, v) \cdot FT t(u, v) + H_{mf}(u, v) \cdot FT \rho(u, v) \} \dots (\text{eq.6})$$

vi. Perform an inverse logarithmic operation using the exponential function.

$$H_{mf} I_M = \exp(FT I_m(x, y)) \dots (\text{eq.7})$$

The next section presents the computational steps incorporated in optimizing the Homomorphic filter generated for enhancing the brain MR image, which is constructed in three different steps is as follows:

## Computing Procedure for Homomorphic filtering

This section illustrates computing steps for applying Homomorphic filtering operation on the input image followed by three sequential steps such as Constructing filter, Applying Constructed Homomorphic filter on the input image, and Homomorphic optimization filter.

### i). Constructing Homomorphic filter

Step-22. Load  $\rightarrow I_m$

a. Go to Step1 to Step5

Step-23. Initialize variable  $\alpha_{Lf}, \alpha_{Hf}$  (low and high-frequency gain),  $f_{odr}$  (filter order)

Step-24. Assign a value for  $f_{odr}$

a.  $f_{odr} \rightarrow \text{Select from the range of 0.5 to 5}$

Step-25. Compute the size of the image

a.  $I_m(\text{Size}) \rightarrow [\text{row} \times \text{colm}]$

Step-26. Compute Homomorphic filter ( $H_{mf}$ )

a. Create an array  $A$  of zeros as per the dimension of the image

b. Compute  $A$

c. Construct Homomorphic filter( $H_{mf}$ )

### ii). Applying Constructed Homomorphic filter on the input image

Step-27. Apply Homomorphic filter-( $H_{mf}$ ) on  $I_m$

Step-28. Assign a value of  $\alpha_{Hf}, \alpha_{Lf}$

a.  $\alpha_{Hf}, \alpha_{Lf} \rightarrow \text{Select between a range of 0.05 to 2}$

Step-29. Compute Homomorphic filtered image-( $H_{mf} \cdot I_m$ )

a.  $H_{mf} \rightarrow ((\alpha_{Hf} - \alpha_{Lf}) \times H_{mf}) + \alpha_{Lf}$

b.  $H_{mf} \rightarrow H_{mf} - 1$

Step-30. Calculate log of  $I_m - (I_m \text{LOG})$

Step-31. Calculate DFT of  $I_m \text{LOG}$

Step-32. Assign filtering on DFT  $I_m$

Step-33. Perform inverse of DFT on filtered  $I_m$

Step-34. Perform inverse log

Step-35. Perform Step-10 and Step-11

Step-36. Display  $H_{mf} \cdot I_m$

### iii) Optimization of Homomorphic filtered image

Step-37. Initialize variable as in Step-12

Step-38 Create an empty matrix as in Step-13

Step-39 Initialize  $kx$  to store all possible values of  $f_{odr}$

Step-40. for  $\alpha_{Hf}, \alpha_{Lf}, f_{odr}$

Step-41. Assign value with a specified range

a.  $\alpha_{Lf} \rightarrow 0.8 \text{ to } 1.1$

b.  $\alpha_{Hf} \rightarrow 0.8 \text{ to } 1.1$

c.  $f_{odr} \rightarrow 0.5$  to 6  
 Step-42. Compute  $H_{mf}$ -  $I_m$  using  $\alpha_{Hf}$ ,  $\alpha_{Lf}$ ,  $f_{odr}$  and  $I_m$   
 Step-43. Compute Accuracy outcome  
 a. GCF, CPP, Contrast, Sharpness  
 Step-44. Assign a value of computed Accuracy outcome into Empty Matrix (Step-38)  
 a.  $v1 \leftarrow GCF$   
 b.  $v2 \leftarrow CPP$   
 c.  $v3 \leftarrow Contrast$   
 d.  $v4 \leftarrow Sharpness$   
 Step-45. Assign value Computed  $\alpha_{Hf}$ ,  $\alpha_{Lf}$ ,  $f_{odr}$  with respect to  $v1$ ,  $v2$ ,  $v3$ ,  $v4 \rightarrow T$   
 Step-46. Perform Reconstruction of  $v1$ ,  $v2$ ,  $v3$ ,  $v4$   
 Step-47. Select an optimal mechanism  
 a.  $V \rightarrow [v_{R1}; v_{R2}; v_{R3}; v_{R4}]^T$   
 b.  $S \rightarrow fs(V, 2)/4$   
 Step-48. Compute fine indexing( $f_i$ )  
 a.  $F_i \rightarrow fmax(S)$   
 b.  $f_{odr} \rightarrow T(f_i, 1)$   
 c.  $\alpha_{Lf} \rightarrow T(f_i, 1)$   
 d.  $\alpha_{Hf} \rightarrow T(f_i, 1)$   
 Step-49. Compute  $H_{mf}$ - $I_m \rightarrow$  Repeat process as shown in Step-29 to Step-34  
 Step-50. Perform Normalization  $\leftarrow H_{mf}$ - $I_m$   
 Step-51. Compute Accuracy  $\rightarrow$  GCF, CPP, Contrast, Sharpness

#### 4. Software and Database.

The design of the proposed framework is implemented in the MATLAB R 2015 b computing environment. MatLab has

various modules for file manipulation, image editing, image analysis, spatial domain enhancement, frequency domain enhancement, and wavelet domain enhancement. MATLAB has a wide variety of function libraries, with a friendly interface, rich functions, and simple operation. This version of Matlab has Image Processing Toolbox containing the features like Gabor and box filtering, C code generation for 20 functions with MATLAB Coder, and improved grayscale morphology and filtering performance

The proposed study uses a brain CTS dataset obtained from the Kaggle database, which can be accessed from "https://www.kaggle.com/datasets" designed as an open repository of task brain CTS images and other data also. Data is available without a registration or license agreement, and by default, data is distributed using a Public Domain license. The Kaggle datasets can be utilized to address or verify many problems related to the human brain. D. Sculley is the CEO at Kaggle database.

#### 5. Results and Discussion

Table-1 illustrates the visualization of the input image and visualization of the computed gamma-corrected image. The obtained gamma-corrected image has better visual quality than the input image. The numerical observation is also given in Table-1 to assess and analyze the gamma correction mechanism's performance in GCF, CPP, Contrast, and Sharpness.

Table-1: Numerical observation of input image and gamma-corrected image

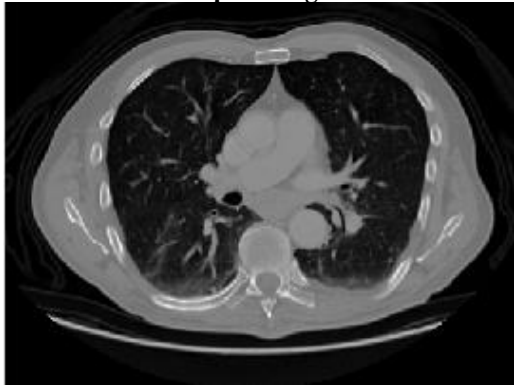

Input Image		Gamma Corrected Image	
			
$\gamma$ - value	--	1.05	
GCF	11.7666	15.6599	
CPP	6.2736	13.7312	
Contrast	2.9999	6.2419	
Sharpness	9.0403	11.1472	

Table-2 demonstrates the different accuracy values with respect to different gamma values (Step17).

Table-2: Illustration of T (table)

Gamma Value ( $\gamma$ )	v1- (GCF)	v2- (CPP)	v3- (Contrast)	v4- (Sharpness)
0.9	7.02	2.24	1.01	3.21
0.95	8.02	3.53	1.35	4.12

1	9.10	4.04	2.03	5.66
1.05	9.96	4.99	2.98	6.91
1.10	11.65	6.01	3.68	9.11
1.15	13.02	7.17	4.24	10.76
1.2	13.94	8.21	4.72	11.67



Finally, gamma-corrected optimization is achieved using in Table-3. and Table-4 shows the same for different input CTS recently computed gamma value (Step-21 and Step-22), shown image.

Table-3: Numerical observation of the optimized gamma-corrected image




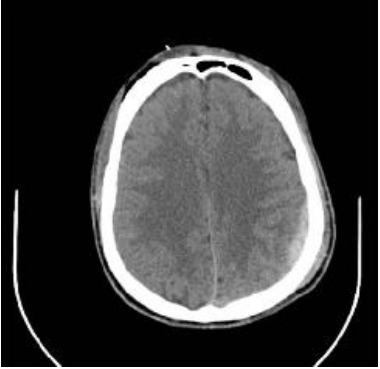
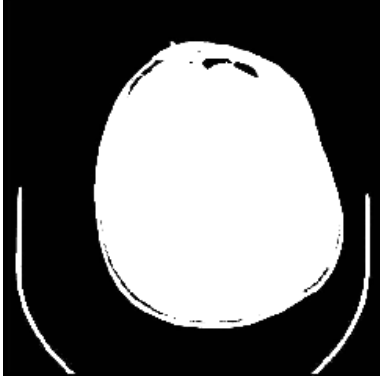
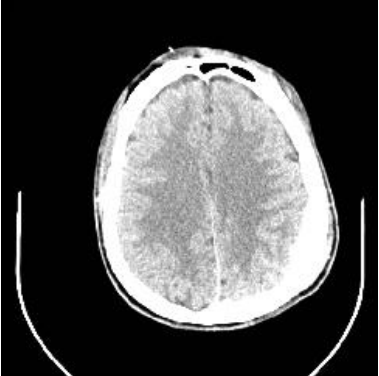
Input Image		Gamma Corrected Image	Optimized Gamma Corrected
			
γ- value	---	1.3 (user selection)	1.2 (optimal)
GCF	11.7666	12.2919	13.7087
CPP	6.2736	6.7369	8.7660
Contrast	2.9999	3.2568	4.1227
Sharpness	9.0403	9.6937	11.2728

Table-4: Numerical observation of the optimized gamma-corrected different brain CTS image

Input		Gamma Corrected	Optimized Gamma Corrected
			
γ- value	---	1.8 (user selection)	1.2 (optimal)
GCF	10.5692	9.6605	9.7901
CPP	9.5736	12.3602	9.7723
Contrast	3.9999	5.3879	4.4387
Sharpness	7.5040	3.0441	6.5348

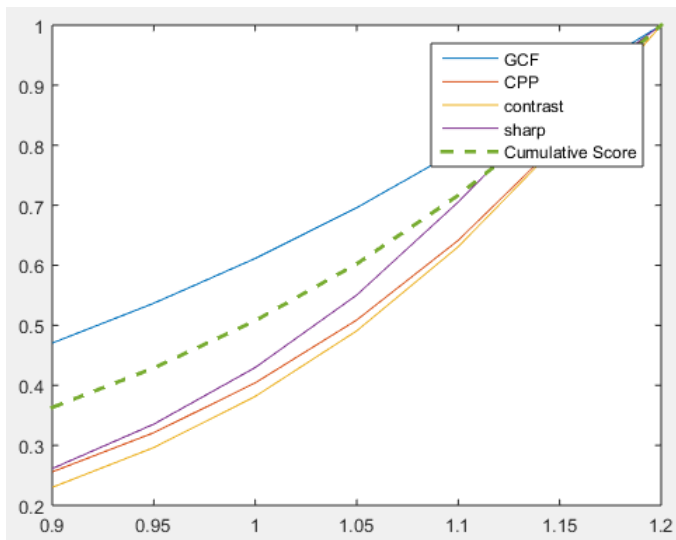


Figure-2: Plot of computation parameters for the Gamma correction method

In the Gamma Correction method, the various computation factors used are plotted with the variation of Gamma value is plotted and is shown in the Figure-2. Here the Gamma value is varied from 0.9 to 2.

The Table-5 exhibits the visualization of input image and visualization of computed Homomorphic filtered image using parameter  $\alpha_{Lf} = 0.15$ ,  $\alpha_{Hf} = 1.39$ , and  $f_{odr} = 2$ . It can be seen that the filtered image has better brightness in terms of the increased reflectance effect than the luminance effect. The numerical observation is also given in Table-5 to assess and analyze the gamma correction mechanism's performance in GCF, CPP, contrast, and sharpness.

Table-5: Numerical observation of input image and Homomorphic filtering image

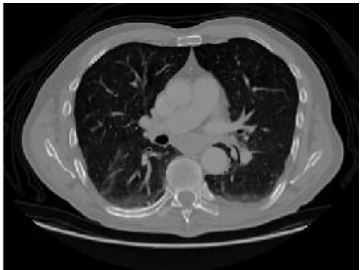

Input Image		Homomorphic Filtered Image		
				
Accuracy	Value	$\alpha_{Lf}=0.0999$	$\alpha_{Hf}=1.02$	$f_{odr}=2$
GCF	11.5020	10.5081		
CPP	8.2736	14.6073		
Contrast	3.027	3.837		
Sharpness	8.0603	9.0213		

Table-6 demonstrates the table's structure as a sample because it is quite impractical to demonstrate such a large dimension (432 x 5) of the table, which contains different accuracy values with respect to different parameter values (Step-45).

Table-6 demonstrates a sample of all possible values computed for  $f_{odr}$  within the range 0.5 to 5  $\alpha_{Hf}$ , and  $\alpha_{Lf}$  within range of 0.8 to 1.1. However, table T has shown only a few randomly selected values from a computed T set because it is challenging to demonstrate here due to its large size, as we already mentioned above. After computing all possible values with different accuracy scores, the proposed system initiates the optimization process. Therefore, the next step towards the optimization process is the reconstruction using function  $f_{max}$  over (v1, v2, v3, v4) (Step-46). After obtaining the

reconstructed v1, v2, v3, and v4, the next process executes to perform a selection of optimal mechanism which is constructed using the transpose of v1, v2, v3, and v4 (equation (8)) to represent them in a column vector for computing sum part of V. The sum part of V is carried out using function  $f_s$  over V which refers to carry a summation of considering specified dimension, i.e., 2 (Step-47). The next important step is executed to compute fine indexing for selecting the optimal value of each parameter for homographic filtering, as shown in computing Step-48. Finally, optimization on the homographic filter image is achieved using the recently computed best indexing parameter and executing prior strategy, i.e., Step-29 to Step-36.

Table-6: Sample Illustration of Table-(T)

$f_{odr}$	$\alpha_{Lf}$	$\alpha_{Hf}$	v1- (GCF)	v2- (CPP)	v3- (Contrast)	v4- (Sharpness)
0.5	0.08	0.08	11.45	5.09	2.62	8.523
1	0.08	0.28	11.54	6.06	3.01	8.792
1.5	0.28	0.08	11.41	5.49	2.50	7.993
2	0.28	0.28	11.62	6.27	3.61	9.021
2.5	0.28	0.08	11.52	5.71	2.45	8.457
3	0.48	0.08	11.48	5.23	2.68	8.271
3.5	0.68	0.28	11.50	6.74	3.39	9.415
4	0.88	0.28	11.57	6.69	3.92	9.621
4.5	0.4	1.08	11.46	12.92	4.26	11.758
5	0.88	1.08	11.71	12.6	4.61	11.924

**Optimization of Homomorphic filtered image:** This process refers to performing an optimization process to achieve optimal  $f_{odr}$  value and another parameter to be applied to the input image to obtain an optimal resolution with bright visibility features. The above presented computational step initializes the v1, v2, v3, v4, and T(table), which is further assigned with the empty matrix having one dimension equivalent to zero and it has no row and column (Step-37 and Step-38). The construction of an empty matrix for the initialized variable can be represented using the equation (4.24).

$v1 = [ ]_{0 \times 0}$  ;  $v2 = [ ]_{0 \times 0}$  ;  $v3 = [ ]_{0 \times 0}$  ;  $v4 = [ ]_{0 \times 0}$  and  $T = [ ]_{0 \times 0} \dots$  (eq.4.24)

Table-7 identified that the optimized image had increased brightness considering optimal value for each parameter, i.e.,  $\alpha_{Lf}=0.08$ ,  $\alpha_{Hf}=1.08$  and  $f_{odr}=5$ . Moreover, it can also be analyzed that there is no significant difference between the GCF parameter of non-optimized filtered images and optimized filter images. However, other accuracy parameters such as CPP, contrast, and sharpness have gained higher scores than the accuracy score of both input and non-optimized Homomorphic filtered images. Table-8 shows the same for different input brain CTS image.

Table-7: Numerical observation of input image and Homomorphic filtering image




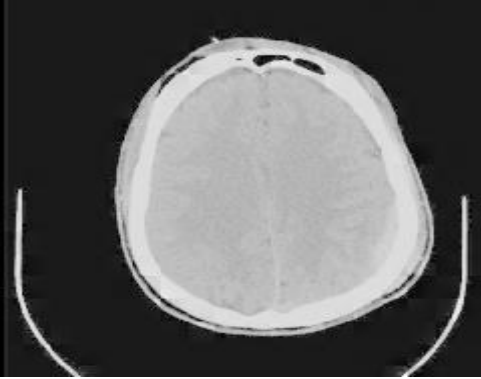
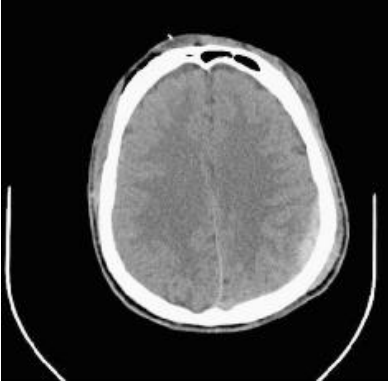
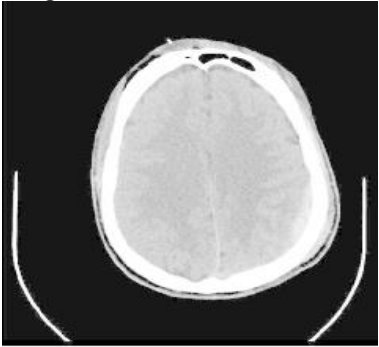
Input		Homomorphic Filtered Image			Optimized Homomorphic Filtered Image		
							
Accuracy	Value	$\alpha_{Lf}=0.8$	$\alpha_{Hf}=1.8$	$f_{odr}=3$	$\alpha_{Lf}=0.18$	$\alpha_{Hf}=1.18$	$f_{odr}=5$
Input Image		User Selection			Optimal		
GCF	11.8692	8.6746			7.9434		
CPP	8.5736	7.9823			12.1677		
Contrast	2.9999	3.5854			4.1776		
Sharpness	8.0403	4.7068			4.1463		

Table-8 Numerical observation of input image and Homomorphic filtering for different brain CTS image

Input		Homomorphic Filtered Image			Optimized Homomorphic Filtered Image		
							
Accuracy	Value	$\alpha_{Lf}=0.8$	$\alpha_{Hf}=1.8$	$f_{odr}=3$	$\alpha_{Lf}=0.18$	$\alpha_{Hf}=1.18$	$f_{odr}=5$
Input Image		User Selection			Optimal		
GCF	11.8692	8.6746			7.9434		
CPP	8.5736	7.9823			12.1677		
Contrast	2.9999	3.5854			4.1776		
Sharpness	8.0403	4.7068			4.1463		

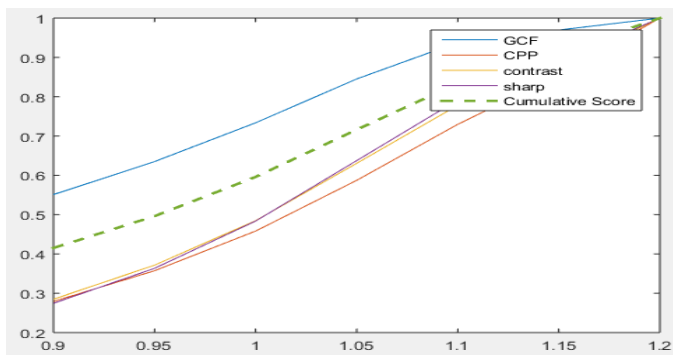


Figure-3: Plot of computation parameters for the Homomorphic Filtering method

In the Homomorphic Filtering method, the various computation factors like GCF – Global Contrast Factor, CPP – Contrast Per Pixel, Contrast, and Sharpness are plotted with the variation of Homomorphic filter order is plotted and is shown in the Figure-3.

From the Figure-2 and Figure-3, it is observed that the computation parameters are having higher values for the Homomorphic filtering method when compared to the Gamma correction method. This results in more efficient pre-processing for the brain CTS images. Thus, Homomorphic Filtering method is better approach for pre-processing brain CTS images, when compared to Gamma Correction method.

## 6. Conclusion:

In this study, we analysed the efficacy of various biomedical filter parameters using CT images, with a particular focus on the Gamma correction method and Homomorphic filtering.

The Gamma correction method proved to be highly effective in enhancing the visibility of CT images. By adjusting the gamma value, we were able to manipulate the luminance of the image, thereby improving the contrast and highlighting important

anatomical structures. The optimal gamma values varied depending on the specific requirements of the image, such as the need for more detailed views of soft tissues or bone structures. Our findings suggest that Gamma correction is a versatile tool that can be fine-tuned to meet the diagnostic needs of radiologists, enhancing their ability to identify and analyze critical medical conditions.

Homomorphic filtering, on the other hand, provided a robust approach to simultaneously enhance contrast and reduce multiplicative noise, which is often a challenge in biomedical imaging. By transforming the image into the logarithmic domain, separating the illumination and reflectance components, and applying filtering techniques, we achieved significant improvements in image clarity. This method was particularly beneficial in standardizing the lighting conditions across the image, thereby enhancing the consistency and reliability of the diagnostic information extracted from the CT scans.

Overall, both Gamma correction and Homomorphic filtering demonstrated substantial benefits in the context of biomedical image enhancement. Gamma correction offered flexible contrast adjustments, while Homomorphic filtering effectively addressed issues related to lighting and noise. Future research could focus on integrating these methods into automated diagnostic systems, further optimizing their parameters for specific medical applications, and exploring their combined use to maximize image quality. Our study underscores the importance of these techniques in advancing the accuracy and efficiency of medical diagnostics through improved imaging technologies.

## References

1. D. Nurhayati and B. Surarso, "Filter Selection and Feature Extraction to Distinguish Types of CT Scan Images," 2021 4th International Seminar on Research of Information



- Technology and Intelligent Systems (ISRITI), Yogyakarta, Indonesia, 2021, pp. 80-85, doi: 10.1109/ISRITI54043.2021.9702847.
2. S. Anitha, L. Kola, P. Sushma and S. Archana, "Analysis of filtering and novel technique for noise removal in MRI and CT images," 2017 International Conference on Electrical, Electronics, Communication, Computer, and Optimization Techniques (ICECCOT), Mysuru, 2017, pp. 1-3, doi: 10.1109/ICECCOT.2017.8284618.
  3. T. Huang, B. Li, S. Tang, Y. Xu, J. Shen and J. Qu, "Reduction of Windmill Artifacts in Helical X-ray CT Images Based on Dual-domain Filtering and Improved Distance Transform," 2021 International Conference on Control, Automation and Information Sciences (ICCAIS), Xi'an, China, 2021, pp. 705-710, doi: 10.1109/ICCAIS52680.2021.9624544.
  4. R. S. Jeena and S. Kumar, "A comparative analysis of MRI and CT brain images for stroke diagnosis," 2013 Annual International Conference on Emerging Research Areas and 2013 International Conference on Microelectronics, Communications and Renewable Energy, Kanjirapally, India, 2013, pp. 1-5, doi: 10.1109/AICERA-ICMiCR.2013.6575935.
  5. S. Cho et al., "A Novel Low-Dose Dual-Energy Imaging Method for a Fast-Rotating Gantry-Type CT Scanner," in IEEE Transactions on Medical Imaging, vol. 40, no. 3, pp. 1007-1020, March 2021, doi: 10.1109/TMI.2020.3044357.
  6. Q. Wu et al., "Unsharp Structure Guided Filtering for Self-Supervised Low-Dose CT Imaging," in IEEE Transactions on Medical Imaging, vol. 42, no. 11, pp. 3283-3294, Nov. 2023, doi: 10.1109/TMI.2023.3280217.
  7. S. H. Malik, T. A. Lone and S. M. K. Quadri, "Contrast enhancement and smoothing of CT images for diagnosis," 2015 2nd International Conference on Computing for Sustainable Global Development (INDIACom), New Delhi, India, 2015, pp. 2214-2219.
  8. W.-J. Zhang, X. Hu, C.-H. Liu, S.-H. Peng, J.-M. Zhao and C.-R. Zou, "A Homocentric Squares Filter for pulmonary nodule enhancement based on the CT images," 2015 8th International Congress on Image and Signal Processing (CISP), Shenyang, China, 2015, pp. 408-412, doi: 10.1109/CISP.2015.7407914.
  9. R. S. Priya, K. L. Narayanan, B. V. Nirmala and R. S. Krishnan, "A Hybrid Deep Learning based Classification of Brain Lesion Classification in CT Image using Convolutional Neural Networks," 2023 Third International Conference on Artificial Intelligence and Smart Energy (ICAIS), Coimbatore, India, 2023, pp. 1426-1431, doi: 10.1109/ICAIS56108.2023.10073907.
  10. Z. Bian et al., "Spatio-temporal Constrained Adaptive Sinogram Restoration for Low-dose Dynamic Cerebral Perfusion CT Imaging," 2018 IEEE Nuclear Science Symposium and Medical Imaging Conference Proceedings (NSS/MIC), Sydney, NSW, Australia, 2018, pp. 1-3, doi: 10.1109/NSSMIC.2018.8824714.
  11. Makeev and S. J. Glick, "Low-Dose Contrast-Enhanced Breast CT Using Spectral Shaping Filters: An Experimental Study," in IEEE Transactions on Medical Imaging, vol. 36, no. 12, pp. 2417-2423, Dec. 2017, doi: 10.1109/TMI.2017.2735302.
  12. Anitha S and Dr B S Nagabhushana (2012), "image compression over low channel bandwidth", second international conference on computer science, engineering and information technology" CCSIT, Part III, LNICST, pp.261.
  13. Speckle noise reduction in ultrasound images – a review Shruthi B,S Renukalatha ,M Siddappa Dept .of computer science and engineering. Sri Siddhartha institute of technology, Tumkur ,Karnataka, India.
  14. MRI medical image de-noising by fundamental filters- Hanafy M.Ali , computers and systems engineering department, faculty of engineering, minia university , El Minia..
  15. J.Rajeesh, R.S.Moni, S.Palanikumar and T. Gopalakrishnan " noise reduction in magnetic resonance images using wave atom shrinkage" International journal of image processing(IJIP), volume(4): Issue(2)2010.
  16. Charles boncelet (2005). "Image noise models ".in Alan C.Bovik. Handbook of image and video processing.
  17. Despeckling of medical ultrasound image Oleg V. Michailovich and Allen Tannenbaum, Member, IEEE.
  18. S. Harish, C. Anil Kumar, Lakshmi Shrinivasan, S. Rohith, Belete Tessema Asfaw, "Algorithm for Recognition of Movement of Objects in a Video Surveillance System Using a Neural Network", Journal of Engineering, vol. 2022, Article ID 8216221, 4 pages, 2022.
  19. Harish. . S., R. . Verma, G. K. . Venkatesh, L. . Vaishnavi D. A., and A. . Kumar C., "Intelligent Filtering Techniques for Reducing Various Noise in Image of Mango Leaves. ", Int J Intell Syst Appl Eng, vol. 12, no. 4s, pp. 367–374, Nov. 2023.
  20. S.A. Akar,"determination of optimal parameters for bilateral filter in brain MR image De-noising " ,Applied soft computing 43(2016)87-96,2016
  21. Noise removal and filtering techniques used in medical images: Nalin Kumar and M.Nachamai, Department of computer science Christ University, Bangalore, India.
  22. Ankush Srivastava, "Comparative study of salt and pepper filters and gaussian filters"
  23. Govindaraj. v, Sengottaiyan, "survey of image denoising using different filter", ijeset volume 2,issue 2,february 2013
  24. J.J.Francis, g.de jager. "the bilateral median filter" iee transaction on image processing,2008 devanand bhonsle, vivek chandra, g.r.sinha, "medical image denoising using bilateral filter" ijigsp,2012